

Lakes' state and abundance across the Tibetan Plateau

Guoqing Zhang · Tandong Yao · Hongjie Xie ·
Kexiang Zhang · Fujing Zhu

Received: 5 November 2013 / Accepted: 19 February 2014 / Published online: 4 April 2014
© Science China Press and Springer-Verlag Berlin Heidelberg 2014

Abstract Understanding the changes in number and areal extent of lakes, as well as their abundance and size distribution is important for assessments of regional and global water resources, biogeochemical cycles, and changes in climate. In this study, changes in lake area greater than 1 km² are mapped using Landsat datasets, spanning the 1970s, 1990, 2000, and 2010. In addition, high-resolution images (GeoCover Landsat mosaic 2000, with a pixel size of 14.25 m) are used for the first time to map lakes as small as 0.001 km² across the entire Tibetan Plateau (TP). Results show that the numbers and areal extent of individual lakes >1 km² in size show a slight decrease between the 1970s and 1990, followed by a clear increase from 1990 to 2010. Ninety-nine new lakes are identified between the 1970s and 2010, 71 of which are found between 1990 and 2010. This indicates the accelerated glacier melt and/or increased difference of precipitation minus evaporation since the 1990s. More than 80 % of the lakes show an increase in their area between the 1970s and 2010. The lake census, using 2000 imagery, shows that there are 32,843 lakes with a total area of 43,151.08 ± 411.49 km², which makes up 1.4 % of the total area of the TP. Around 96 % of all lakes are small, with an area

<1 km², while the 1,204 large lakes (>1 km²) account for 96 % of the total lake area. The TP is subdivided into 12 greater drainage basins, and of these the inner TP dominates in terms of the number of lakes (55.03 %), the total area of lakes (66 %), and lake density (0.026/km² compared to the mean, 0.011/km²). A plot of lake abundance against size shows that the size distribution of lakes departs from a typical power-law distribution, but displays such a distribution at the mean elevation (4,715 m), with an r^2 value of 0.97 and a slope of -0.66. The slopes of the abundance-size equations from each of the 12 greater basins, and from all basins together, are larger than -1, supporting the inference that larger lakes, rather than the small lakes, contribute more to the total lake surface area across the TP. The lake inventory provided in this study, along with the assessment of lake size distribution, have important implications for estimates of water balance, for water resource management, and for lake area estimations in the TP.

Keywords Lake area · Size distribution · Abundance · Tibetan Plateau · Landsat

G. Zhang (✉) · T. Yao
Key Laboratory of Tibetan Environmental Changes and Land Surface Processes, Institute of Tibetan Plateau Research, Chinese Academy of Sciences, Beijing 100101, China
e-mail: guoqing.zhang@itpcas.ac.cn

H. Xie
Laboratory for Remote Sensing and Geoinformatics, University of Texas at San Antonio, San Antonio, TX 78249, USA

K. Zhang · F. Zhu
Jiangxi Provincial Key Laboratory for Digital Land, East China Institute of Technology, Nanchang 330013, China

1 Introduction

Lakes are known to affect regional climate, exchanging heat and water with the atmosphere [1]. The emission of greenhouse gasses from lakes is one of the essential components of the global carbon cycle, also potentially regulating climate change [2, 3]. Lake abundance is a metric used to describe the number of lakes larger than or equal to a given size [4]. The abundance and size distribution of lakes, therefore, play a significant role in regional and global biogeochemical cycles [5–7].

Downing et al. [7] suggested that the actual global lake area is twice as large as has been previously estimated, and is dominated by lakes with an area smaller than 1 km^2 , based on extrapolations from power-law size distributions. McDonald et al. [6], however, analyzed 3.5 million lakes and reservoirs in the United States and concluded that the number of small lakes could be overestimated by power laws such as the Pareto distribution. Further, Seekell and Pace [8] found that in some regions, the power-law distribution does not apply when small-sized lakes are considered. In addition, while lakes in flat regions typically follow a power-law size distribution, those in mountainous regions do not [5, 9]. An analysis of global primary production in lakes has demonstrated that power-law distributions greatly overestimate lake distribution, by around 45 %, compared to non-power law distributions [10]. As such, our motivations for this study is to address (1) the number and areal extent of lakes across the entire Tibetan Plateau (TP), and how these attributes have changed; and (2) if the lakes follow a power-law distribution?

Most of the world's lakes are thought to exist in glacialized terrains [11], and the total area of glaciers on the TP and its surrounding area is around $100,000 \text{ km}^2$ [12, 13]. The lake areas and water levels tend to increase as climate warms, accompanying an accelerated retreat of glaciers and an increase in net precipitation [12, 14–24]. Under such a scenario, new glacial lakes would appear, resulting in thousands of small, unidentified lakes. The smaller lakes typically dominate in terms of total number [6], and an understanding of their extent is crucial for evaluating regional lake characteristics and biogeochemical processes [3, 8, 25].

Lakes on the TP are rarely influenced by human activities, and are, therefore, the representative of natural water bodies. Several lake investigations have been carried out on the TP [26–29]. For example, Wang and Dou [27] conducted the first lake census on the TP, spanning the 1960–1980s, and reported that there are 1,091 lakes with an area greater than 1 km^2 . A more detailed lake survey in China in 2005–2006 showed that most of the 30 newly identified lakes and many with an increase in size are located on the TP [26, 28]. However, these two studies have focused only on the changes in lake characteristics in the Tibet Autonomous Region and Qinghai Province (Fig. 1). In addition, many studies have only reported the changing number and sizes of specific lakes or lake groups in a particular watershed [24, 30–32], or of large lakes with an area of $>10 \text{ km}^2$ [33]. Currently, changes in lake characteristics across the entire TP remain unknown.

In the present study, the boundary of the TP is derived from the Shuttle Radar Topography Mission Digital Elevation Models (SRTM DEMs; Fig. 1). Within TP, lakes larger than 1 km^2 are identified in data from the 1970s,

1990, and 2010. In particular, orthorectified Landsat Enhanced Thematic Mapper plus (ETM+) mosaics from the GeoCover circa 2000, with a pixel size of 14.25 m , provide an unprecedented opportunity to identify small lakes across the TP. This study provides the first detailed lake inventory of the TP, as well as an evaluation of the lake size distribution in this area. These analyses further enrich the global lake database, as well as enhance the water balance estimations of lakes, adding to previous studies carried out on large lakes [4, 18, 19, 33]. In addition, the results have important implications for limnological analyses and climate change studies of the TP.

2 Data and methodology

2.1 SRTM DEM and outlining the TP and basins

The SRTM collected a near-global (56°S to 60°N) elevation database during an 11-d mission in February 2000 [34]. The resulting SRTM DEM with a 90-m pixel size has been widely used to delineate watersheds and basin boundaries, in addition to the shorelines of water bodies such as lakes, rivers, and oceans [18, 35]. We define the boundary of the TP using SRTM v4.1 data above the elevation of $2,500 \text{ m a.s.l.}$ (Fig. 1). The total area of the TP based on this boundary is $3.08 \times 10^6 \text{ km}^2$. In addition to this, the TP can be subdivided into some large basins, using a suite of drainage and water flow datasets developed from the SRTM DEM (<http://hydrosheds.cr.usgs.gov/>). Furthermore, the elevations of the lake's surfaces are also extracted from the SRTM data.

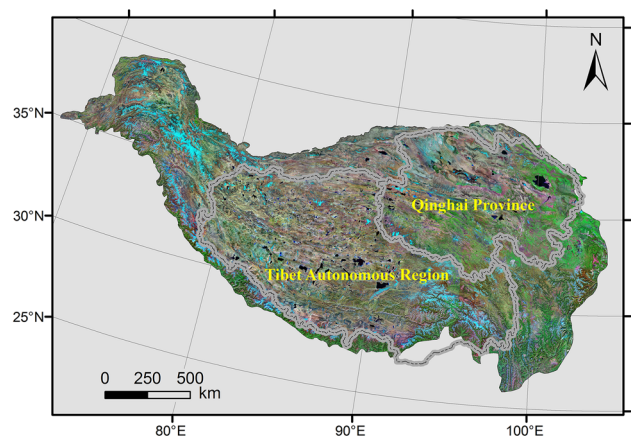


Fig. 1 Lake distribution across the TP. The boundary of TP is extracted from SRTM DEM. The boundaries of Tibet Autonomous Region and Qinghai Province are also shown. The background is Landsat ETM+ GeoCover mosaics circa 2000

2.2 Landsat data and lake area extraction

Landsat imagery is among the most widely used remote sensing data sources for the extraction of surface water information. The Landsat GeoCover mosaics with minimal cloud coverage ($\leq 10\%$) are presently the best available datasets for global land mapping [36]. The global orthorectified and co-registered Landsat Multispectral Scanner (MSS), Thematic Mapper (TM), and ETM+ data are produced by NASA for three separate periods: the late 1970s, circa 1990, and circa 2000 [36]. The circa 1990 and 2000 time periods comprise 85,000 Landsat TM/ETM+ scenes, which were acquired in 1990 ± 3 years and in 2000 ± 3 years. These datasets are geo-referenced using the Universal Transverse Mercator (UTM) coordinate system and World Geodetic System 1984 (WGS1984) data. Three Landsat TM/ETM+ bands (2, 4, and 7) are sharpened with the panchromatic band using a cubic-convolution process [37] to provide a product with a pixel size of 28.5 m for 1990 and of 14.25 m for 2000, with a positional accuracy of 50 m (RMSE) in GeoTIFF format. These datasets from circa 1990 and 2000 are available from the University of Maryland's Global Land Cover Facility (<http://glcf.umd.edu/data/mosaic/>). In this study, a total of 17 GeoCover mosaics from circa 1990 and 2000 are used, covering the entire TP (Table 1).

In addition, 114 scenes from the Landsat MSS in the 1970s (from 1972 to 1978), and from ETM+ around October, 2010 with the minimum cloud cover are also used (Table 1). The Landsat MSS and ETM+ have spatial resolutions and mean cloud coverage of 80 m and 7.2 %, and 30 m and 8.6 %, respectively. These data sets are provided by the U.S. Geological Survey (USGS) (<http://glovis.usgs.gov/>) and the Geospatial Data Cloud, Computer Network Information Center, Chinese Academy of Sciences (<http://www.gscloud.cn>).

In this study, all remote sensing data used for the extraction of lake area are derived from Landsat data sets, which have been widely used for surface water mapping. The Landsat images selected for this study are from the LIT product, which has been geometrically corrected (<http://landsathandbook.gsfc.nasa.gov/>). The Landsat ETM+ has a data gap from May 31, 2003, due to a scan line corrector failure. The gaps of Landsat ETM+ data used for

this study are filled using a local linear histogram-matching method developed by [38].

A few algorithms for automated water extraction have been developed [39, 40]. Among these, single-band thresholding and spectral water indices are commonly used for the extraction of water from visible and infrared imagery [40, 41]. However, these methods still require manual examination and editing after the automated water body detection. In particular, environmental factors on the TP, such as masses of clouds, snow and glaciers, and shadows, can complicate the classification process. In addition, many lakes and rivers are connected, thus it is not easy to reliably separate them using an automated approach. As a result, digitization through visualization with prior knowledge is used in this study to map the lakes. Although this is a very time-consuming process, especially over such a large region, this method permits examination of lake boundaries with the best quality control, while consistent throughout the four examined imagery periods.

The original Landsat Mosaics 1990/2000 and MSS/ETM+ are referenced to a UTM projection. The false color composites are used to combine the three Landsat bands (754 for MSS and 543 for ETM+ as RGB red, green, and blue) through ENVI v4.8. The lakes within each scene image are visually interpreted and digitized in ArcGIS, and the vector lake data are then projected onto an Albers Conical Equal Area coordinate system, and combined together. If cloud and snow cover a lake boundary, several scenes of the same region are used to provide an accurate depiction. The preview images provided by the USGS Global Visualization Viewer (<http://glovis.usgs.gov/>) allow rapid examination of cloud and snow conditions before the original Landsat data are downloaded. In order to include all lakes with an area greater than 1 km² in the inventories from the 1970s, 1990 and 2010, almost all lakes visible in the images are delineated in this way.

The accuracy of the extracted lake areas may be controlled by pixel size, image quality as affected by clouds, snow and glaciers and shadow coverage, classification algorithms, and the experience of the researcher. As such, some studies have indicated that the lake boundary can be identified with an error of ± 0.5 pixels either side of the shoreline [42, 43]. Using this, the area uncertainty for each lake is estimated, allowing calculation of the uncertainties of the total lake area in the four study periods.

Table 1 Satellite data used in this study

Data set	Pixel size (m)	Scene size	Coverage date	Number of scenes used	Mean cloud coverage (%)
Landsat MSS	80	185 km \times 185 km	1970s (1972–1978)	114	7.2
GeoCover circa 1990	28.5	5° \times 6°	1990 \pm 3	17	<10
GeoCover circa 2000	14.25	5° \times 6°	2000 \pm 3	17	<10
Landsat ETM+	30	185 km \times 185 km	October, 2010	114	8.6

2.3 Lake size distribution

A number of statistical conclusions can be drawn based on the relationship between lake number and area, using both regional and global lake data sets. All lakes on the TP, representing divergent topography and geology, are included in this examination of lake size distributions. The fractal aspect of the size distribution of lakes at the mean elevation is measured using the following regression [4, 5]:

$$N = cA^{-b}, \quad (1)$$

where N is the number of lakes greater than area A , c is a constant, and b is a parameter describing the logarithmic rate of decline of lake number with increasing lake area [7]. This is similar to the Pareto distribution, which has previously been used to describe lake size-frequency distributions [44]. Theoretical studies suggest that lakes following a power-law distribution are usually constrained by $0.5 \leq b \leq 1$ (or with a slope of $[-1, -0.5]$) [5, 44, 45]. In addition, to accept the distribution, the r^2 value for the log-abundance versus log-size regression must be greater than the critical value at the 0.05 significance level, as provided by [8].

3 Results and discussion

3.1 Changes in lake number and area

A total of 1,924, 1,699, 32,843, and 1,617 lakes are identified and delineated in the 1970s, 1990, 2000, and 2010, respectively. The numbers of lakes with an area of more

than 1 km^2 in the four periods (1970s, 1990, 2000, and 2010) are 1,081, 1,070, 1,204, and 1,236, respectively. The lake numbers identified in the seven separate area divisions (>1 , 1–10, 10–50, 50–100, 100–500, 500–1,000, and $>1,000 \text{ km}^2$), from this study and previous studies, are summarized in Table 2. The number of lakes more than 1 km^2 in area in the 1970s is similar to that found previously during the 1960–1980s [27]. However, the total lake area found for that period [27] is much larger than this study shows; this difference in lake area may be attributed to the inclusion of playas such as the Qarhan Salt Lake ($4,704 \text{ km}^2$) in the former study. The numbers of lakes identified in the Landsat data from 2000 to 2010 in this study, and from the SRTM DEM [18] are much greater than during 2005–2006, as indicated by [26]. This could be a result of the enhanced accuracy and resolution of the multi-mission satellite data, or the different extents of study area (the entire TP, as opposed to just Tibet Autonomous Region and Qinghai Province) in [26]. For comparison, a study mapping lakes from SRTM data in 2000 [18] has an areal extent that is the same as that in the present study. Yet, the current analysis still identified more lakes, amounting to 1,204 compared to the 1,123 lakes using the SRTM data alone. This is, therefore, likely attributed to the high spatial resolution of the data used.

Figure 2 shows the changes in lake shoreline and areas of three of the largest lakes on the TP: Nam Co, Selin Co, and Qinghai Lake. Nam Co and Selin Co show a continuous expansion between the 1970s and 2010. In particular, the area of Selin Co in 2010 is notably larger ($2,349 \text{ km}^2$) than that of Nam Co ($2,026 \text{ km}^2$), which was previously known as the largest lake in Tibet. Qinghai Lake shows an

Table 2 Number of lakes in each area division from previous studies, compared to the present study

Area division (km^2)	$>1,000$	500–1,000	100–500	50–100	10–50	1–10	>1	Area ($>1 \text{ km}^2$)	$<1 \text{ km}^2$	Acquired period	Data set	Source
Lake number	5	10	57	69	204	746	1,091	44,993		1960–1980s		[27]
	4	10	55	68	213	731	1,081	$40,126 \pm 1022$		1970s	Landsat MSS	This study
	3	9	64	67	209	718	1,070	$39,671 \pm 394$		1990	Landsat mosaic	This study
	3	9	65	72	237	818	1,204	$41,256 \pm 214$	31,639	2000	Landsat mosaic	This study
	3	7	66	69	218	760	1,123	39,800	3,222	2000	SRTM DEM	[18]
	3	10	68	70	238	666	1,055	41,832		2005–2006	Topographic map, CBERS, Landsat	[26]
	5	9	82	73	255	812	1,236	$47,366 \pm 486$		2010	Landsat ETM+	This study

overall decrease in area between the 1970s and 2010, despite showing a slight increase between 2000 and 2010. It can be clearly seen that the reversal occurred in 2004, from separately acquired annual lake level data [15].

The numbers of lakes and their area changes between the 1970s and 2010, for lakes with areas greater than 1, 10, 50, and 100 km², are shown in Fig. 3. For lakes greater than 1 km² in area, both number and total area decrease, from 1,081 and 40,126 km² in the 1970s to 1,070 and 39,671 km² in 1990. During the last 20 years, however, the lake number and area increase continuously, reaching 1,236 and 47,366 km² in 2010, respectively. The number of lakes with areas greater than 10, 50, and 100 km² shows a consistent increase between the 1970s and 2010, while the total area decreases slightly between the 1970s and 1990, before increasing notably between 1990 and 2010.

The seasonal variations and inconsistency in the dates of acquisition of the Landsat data could result in some uncertainties, due to the limited availability of data. However, seasonal fluctuations in lake area on the TP are small, compared to lakes in the more humid South China region [19, 22]. In addition, we calculate the total lake area for each of the four different study periods, and compared their area changes over time spans of at least 20 years, between the 1970s (1990) and 2010. Thus, seasonal variations are likely to result in only small abnormalities in the data.

3.2 Regional distribution

The spatial distribution of lake changes from the 1970s to 2010, and from 1990 to 2010 is also examined. The TP is subdivided into 12 greater drainage basins, according to the locations of large rivers, as well as geomorphic and geological units; the numbers and sizes of lakes in each basin are recorded. Figure 4 shows that 71 new lakes appeared from 1990 to 2010 (20 years), as compared to 99 new lakes from 1970s to 2010 (40 years). This number is far greater than the 30 new lakes previously reported between the 1960–1980s and 2005–2006 by [28]. The new lakes found in this study are mainly located in the Inner TP (over 50), a closed basin without outflow (Fig. 4).

Lakes showing an increase or decrease in area between the 1970s and 2010 and between 1990 and 2010 are also compared (Fig. 4). Lakes with area changes of less than 1.5 % are considered as unchanged [33]. In total, 925 of the 1,137 lakes (81 %) show expansion of their areas between the 1970s and 2010, and 979 of the 1,165 lakes (84 %) increase in area between 1990 and 2010. Those lakes with an area increase are also mostly distributed in the Inner TP (68 %) (Fig. 4). Among these, the greatest number of lakes, i.e., 35 % between 1970s and 2010 and 27 % between 1990 and 2010, show an area increase of 10 %–

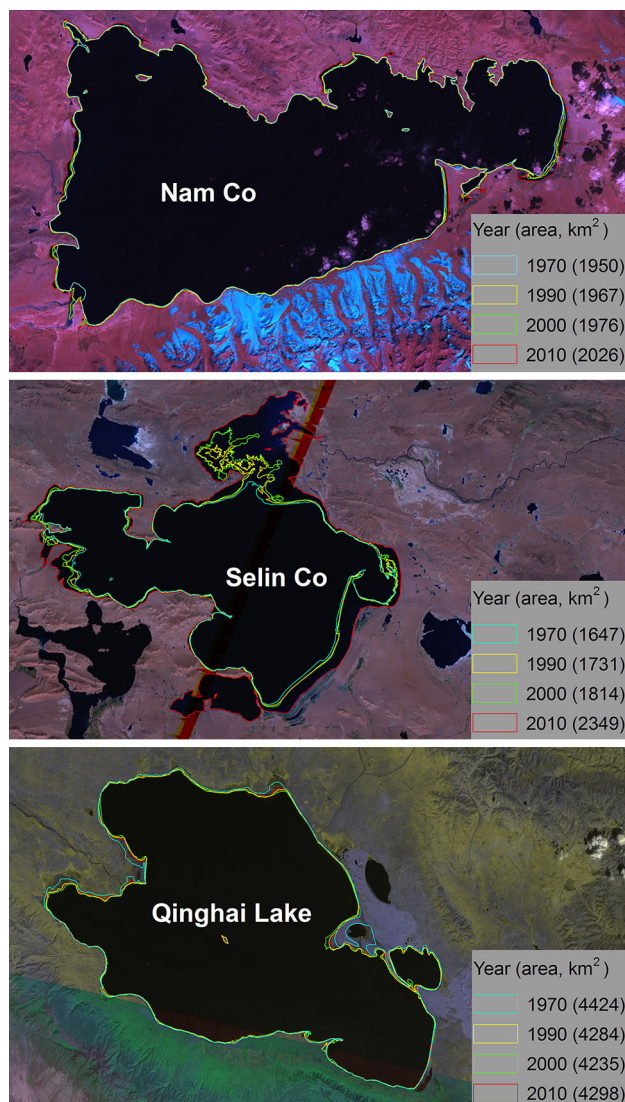


Fig. 2 An example showing the changes in lake shoreline and lake area in the four different periods (1970s, 1990, 2000, and 2010) for Nam Co, Selin Co, and Qinghai Lake

50 %. The general increase in the area of lakes in the past 20 years, especially in the Inner TP, may be attributed to increased inflow of water from melting glaciers [12, 30, 46–48] and precipitation [23, 24, 49]. At present, only Nam Co has been quantitatively evaluated for its water balance with accompanying gage measurement data [31, 50]. Thus, it is still difficult to estimate the relative contributions of glaciers and precipitation to the lake increase across the entire TP, as a result of limited station observations.

Across all of the TP, 212 (19 %) and 186 (16 %) lakes show an area decrease between the 1970s and 2010, and between 1990 and 2010, respectively. These are mostly distributed in the Inner TP and Brahmaputra basins, which contain 44 % and 16 % of the shrinking lakes between the 1970s and 2010, and 30 % and 21 % between 1990 and

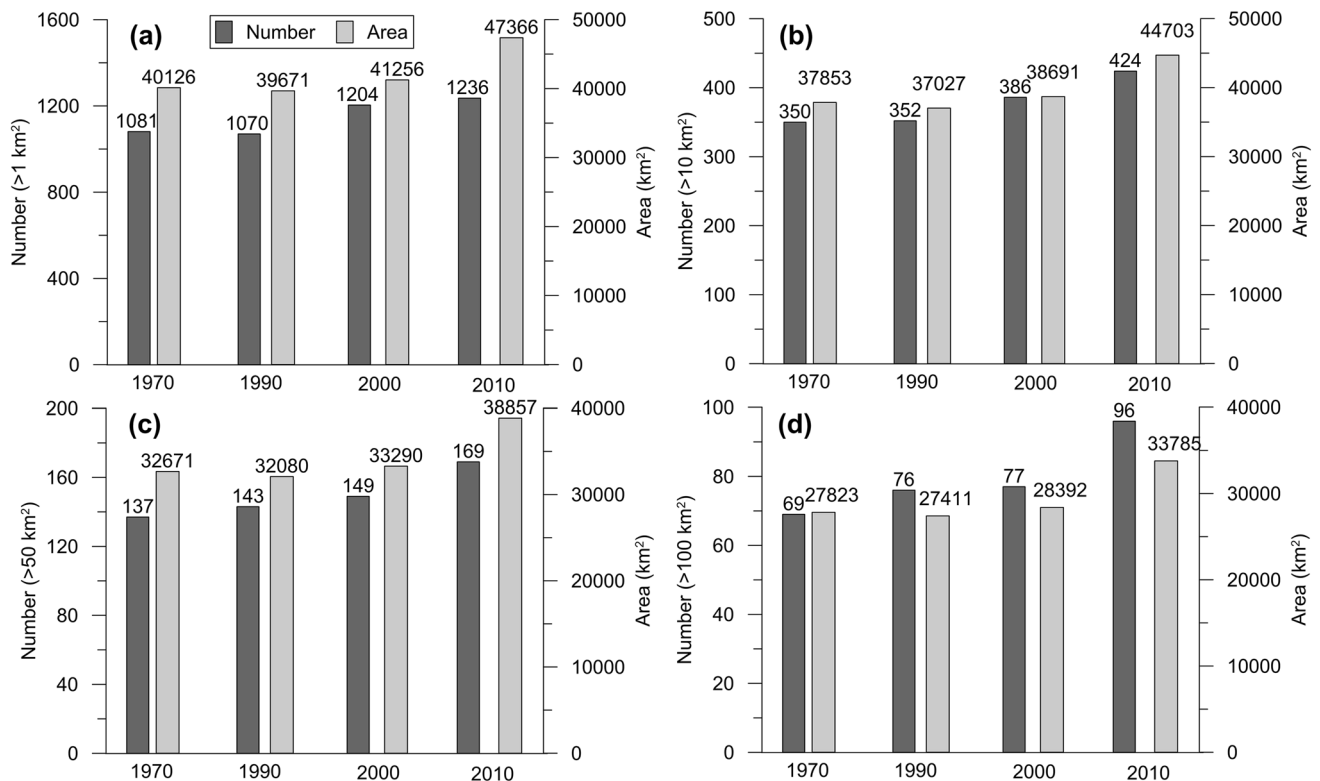


Fig. 3 Lake number and total area for lakes with areas greater than: **a** 1 km², **b** 10 km², **c** 50 km², and **d** 100 km² in the 1970s, 1990, 2000, and 2010, respectively

2010, respectively. Around 50 % of the lakes show an areal decrease of 1.5 %–10 %. Yamzhog Yumco in the Brahmaputra basin is the largest lake showing an area decrease between 1990 and 2010, and has shown the largest lake level decline in recent years [16]. Potential reasons for such a reduction in size are complex, and include negative differences between precipitation and evaporation caused by a warmer climate in the lake basins [32, 51]. In addition, anthropogenic factors such as the Yamzhog Yumco Pump-Storage Power Station may have also contributed to the lake level drop in Yamzhog Yumco [16].

Table 3 shows that there are 32,843 lakes that underwent changes in area, from 0.001 to 4,235 km², as evidenced by circa 2000 ETM+ data sets. Only 1,204 lakes are individually larger than 1 km² each, and thus small lakes dominate in terms of lake number, with 96 % of all lakes having an area less than 1 km². However, large lakes dominate in terms total lake surface area, and the 1,204 large lakes account for 96 % of the total lake area. This is also shown in the inset of Fig. 5.

All of the lakes combined represent a total area of (43,151.08 ± 411.49) km², which represents 1.4 % of the TP's total surface area (3.08 × 10⁶ km²). The mode, mean, and median lake areas are 0.006, 1.31, and 0.021 km², respectively. The lake density for the entire area is 0.011 km⁻². The lakes are mainly located in the Inner TP

(Table 3; Fig. 5), which itself contains 18,075 lakes (55.3 % of the total lake number) and 777 lakes larger than 1 km² (65 % of all lakes >1 km²). In this region, lake area accounts for 4 % of the land area. Furthermore, the Inner TP has a lake density of 0.026 km⁻², which is the highest of all 12 basins.

The median lake size is less variable among the basins, ranging from 0.01 km² for the Ganges River basin to 0.065 km² for the Indus River basin. Several great river basins, such as those of the Yellow River and the Yangtze River, also have a high number of lakes (>10 % of the total, each), while the Amu Darya, Indus River, Salween, and Brahmaputra River basins have a moderate number of lakes (1.5 %–5 %). The Qaidam and Hexi Corridor River basins have a small total lake area, yet their mean lake size is the highest (>5 km²) and the lake density is among the lowest (0.001 km²) of all the basins.

Lake boundaries and sizes are the basic datasets for many applications. For example, Zhang et al. [16] examined the changes in water level of 74 lakes in the TP using 4–7 years ICESat data and lake boundaries delineated from 500-m snow cover products. Phan et al. [20] found 154 lakes with available ICESat data using a 250-m water mask. A recent study showed that 200 lakes can be examined for their changes in water level, using lake boundaries derived from 90-m-SRTM DEM data sets [18]. The present study provides the largest possible lake

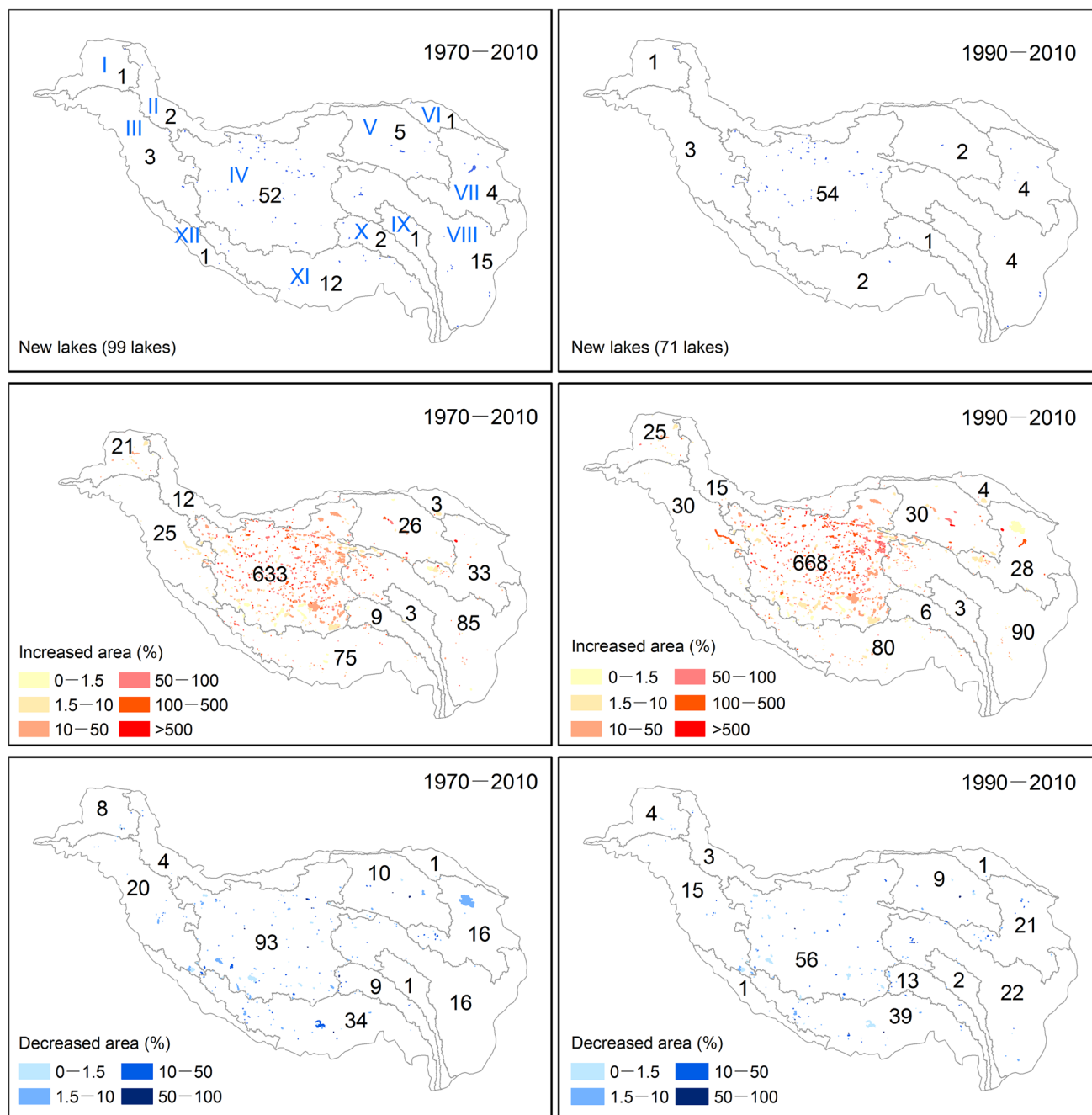


Fig. 4 Lake area changes between the 1970s and 2010 (*left*) and 1990 and 2010 (*right*) in 12 drainage basins of the TP, for newly appeared lakes (*top*), lakes increase in size (*middle*), and lakes decrease in size (*bottom*). The *number* in this figure is the number of lakes in each basin. The names of 12 basins are Amu Darya (I), Tarim (II), Indus (III), Inner TP (IV), Qaidam (V), Hexi Corridor (VI), Yellow (VII), Yangtze (VIII), Mekong (IX), Salween (X), Brahmaputra (XI), and Ganges (XII), respectively

numbers and coverage, which can be used for better extraction of laser or radar footprints over a lake's water surface in future studies.

The latitudinal distribution of lakes is shown in Fig. 6. This shows that most lakes are located between 30°N and 35°N, with the highest concentration of lakes found around latitude 34°N. Globally, lakes are most concentrated

between 50°N and 70°N in glacial areas including Alaska, Canada, and northern Russia [4]. Generally, the latitudinal distribution of lake area is consistent with lake numbers. However, the largest peak in lake area appears at 31°N, mostly as a result of the occurrence of Nam Co and Selin Co at this latitude. The largest lake, Qinghai Lake, is mostly responsible for the secondary peak at around 36°N.

Table 3 Abundance and size distribution of lakes (based on Landsat mosaic 2000) within each of the 12 basins in the TP

Basin name	Basin area (10 ⁵ km ²)	Number of lakes (%)	Lake area, km ² (coverage, %)	Number of lakes (>1 km ²)	Lake area, km ² (>1 km ²)	Mode (km ²)	Mean lake area (km ²)	Median lake area (km ²)	Lake density (lakes km ⁻²)
I	1.26	1,030 (3.14)	748.49 ± 12.98 (0.59)	30	676.32 ± 5.99	0.009	0.73	0.033	0.008
II	1.91	195 (0.59)	98.85 ± 3.16 (0.05)	15	76.65 ± 1.27	0.02	0.51	0.065	0.001
III	3.19	1,638 (4.99)	1,868.73 ± 21.21 (0.59)	50	1,750.87 ± 9.76	0.013	1.14	0.041	0.005
IV	7.08	18,075 (55.03)	28,416.77 ± 255.69 (4.01)	777	27,384.18 ± 145.59	0.006	1.57	0.022	0.026
V	2.53	242 (0.74)	1,362.76 ± 9.08 (0.54)	37	1,346.17 ± 7.56	0.014	5.63	0.036	0.001
VI	0.66	95 (0.29)	597.86 ± 1.45 (0.91)	5	593.10 ± 0.46	0.005	6.29	0.024	0.001
VII	2.50	5,537 (16.86)	6,239.83 ± 35.93 (2.50)	52	6,094.52 ± 13.28	0.005	1.13	0.010	0.022
VIII	4.78	3,661 (11.15)	1,164.56 ± 34.08 (0.24)	101	913.22 ± 10.29	0.006	0.32	0.026	0.008
IX	0.91	187 (0.57)	48.13 ± 1.52 (0.05)	5	39.54 ± 0.46	0.007	0.25	0.023	0.002
X	1.11	554 (1.69)	308.81 ± 5.83 (0.28)	20	266.96 ± 2.03	0.008	0.56	0.036	0.005
XI	4.03	1,549 (4.72)	2,288.32 ± 29.89 (0.57)	112	2,114.53 ± 16.48	0.018	1.48	0.057	0.004
XII	0.86	80 (0.24)	7.97 ± 0.69 (0.01)	0	0	0.011	0.09	0.053	0.001
Total	30.82	32,843	43,151.08 ± 411.49 (1.40)	1,204	41,256.05 ± 213.66	0.006	1.31	0.021	0.011

Basin names (I–XII) are the same as in Fig. 4

The spatial distribution of lakes on the TP is the result of both tectonic movement and interacting hydrological factors. In the interior TP, which is dominated by internal drainage systems, basin filling could have played a major role in smoothing out the tectonically generated structural relief [52, 53]. Lake development on the TP may include several phases, including drying, growing, closing, and salting, which are associated with climate and environmental changes, as well as crustal uplift. For example, Chen et al. [54] have found that Zhari Namco has shrunk over the last 8.2 ka, due to the weakening of the Asian monsoon.

3.3 Lake size distribution

The abundance-size plots for lakes within each basin and for the entire TP are examined, in order to test whether they conform to a power-law distribution. Figure 7 shows that the slope of the regression between log-abundance and log-size in 10 of the 12 basins are within the theoretical constraints (−1 to −0.5). The exceptions to this are the Qaidam and Hexi Corridor basins, which have slope values above the criteria. The *r*² values are all high for the 10 matching basins, ranging from 0.87 to 0.98. However, all are still lower than the critical value at the 0.05 confidence level [8]. This suggests that the size distribution of lakes in each basin of the TP deviates somewhat from a typical power-law distribution.

The lake size distribution for all lakes together in the TP (Fig. 8a) shows a slope of −0.60 and an *r*² value of 0.98, which is slightly lower than the expected value of 0.99 at the 0.05 confidence level, thus indicating conformance to a power-law distribution. The lakes at the mean elevation (4,715 m), however, conform more closely to the power-law distribution, with a slope of −0.66 and an *r*² of 0.97, larger than the required 0.90 at the 0.05 confidence level (Fig. 8b, c).

Lakes on the TP in high mountainous Asia tend to deviate from power-law distributions, which is consistent with previous theoretical work that has suggested that lakes in mountainous regions do not follow a power-law distribution [5]. Typically, however, small lakes are not often recorded on maps, and thus their abundance and size distribution cannot be estimated using the assumption of a power-law distribution, which could result in an overestimation of lake numbers. Although some small lakes remain unknown, the present study has shown that large lakes dominate the total lake area. The high concentration of lakes across the TP, and in particular the smaller lakes, can be attributed to glacier feeding [30, 55–57]. Small lakes react faster to changes in climate more rapidly than large lakes, and would, therefore, be of significance to studies of regional biogeochemical cycles.

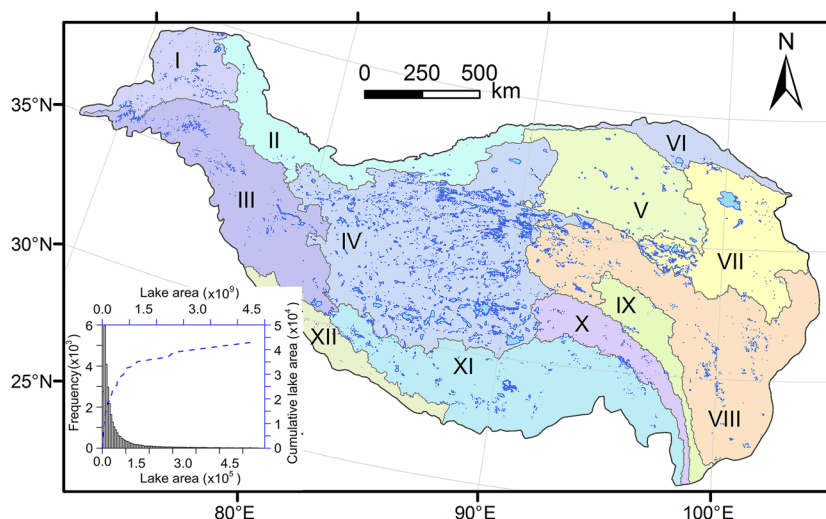


Fig. 5 All lakes across the TP, derived from Landsat ETM+ data circa 2000. Inset shows lake abundance and an area histogram. Basin names (I–XII) are the same as in Fig. 4

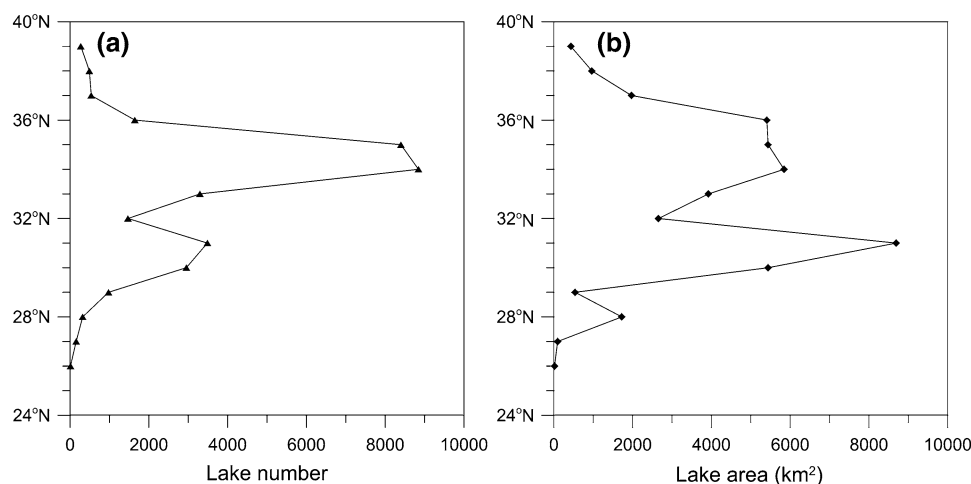


Fig. 6 Latitudinal distribution of lake number (a) and lake area (b) across the TP. Lake number and area are aggregated in steps of 1° latitude

4 Conclusions

The number of lakes across the TP and their respective areas has been examined, using data from the 1970s, 1990, 2000, and 2010. The numbers of lakes and the sum of areas greater than 1 km² are 1,081 and (40,126 ± 1,022) km² in the 1970s, 1,070, and (39,671 ± 394) km² in 1990, 1,204, and (41,256 ± 214) km² in 2000, and 1,236 and (47,366 ± 486) km² in 2010. Total lake area shows slight decrease between the 1970s and 1990, yet both number and area show a continuous increase between 1990 and 2010 in the four different size classes (>1, 10, 50, and 100 km²).

Between the 1970s and 2010, 99 new lakes are found, 71 of which appear between 1990 and 2010. This indicates the accelerated glacier melt and/or increased difference of

precipitation minus evaporation since the 1990s. Of the existing lakes, 80 % show an increase in their area, with 94 % increasing their size by >1.5 % during the two comparison periods. Those lakes with an area increase are mainly distributed in the Inner TP (68 % of the total), and the largest number of lakes experience an area increase of 10 %–50 %. In contrast, lakes showing a decrease in their area are mostly distributed in the Inner TP and Brahmaputra basins. Around 50 % of the lakes with an area decrease had shrunk by 1.5 %–10 % during the study period.

This study provides the first complete lake census for the TP. Lakes ranging in area between 0.001 and 4,235 km² are delineated using Landsat GeoCover mosaics circa 2000 with a spatial resolution of 14.25 m. A total of 32,843 lakes have been delineated across the TP, with a total area of

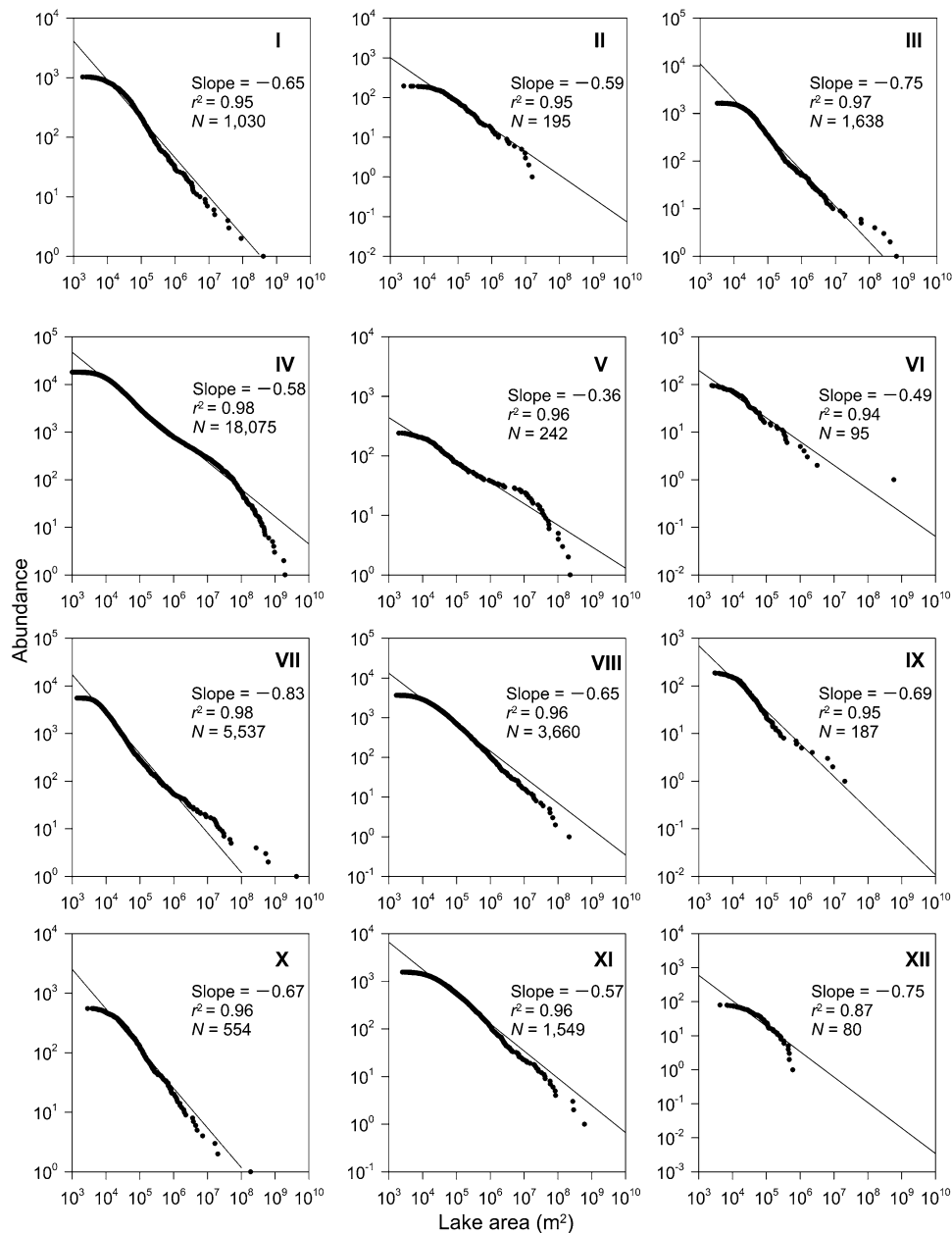


Fig. 7 Plots of log-abundance versus log-size for lakes in each basin of the TP. Basin names (I–XII) are the same as in Fig. 4

(43,151.08 ± 411.49) km² (making up 1.4 % of the total area of the TP). Most of the lakes (96 %) are small, with an area of less than 1 km². We believe that small lakes (<1 km²) should receive more academic attention, as little has been discovered about their abundance and roles, prior to the present study.

The regional distribution characteristics of lakes on the TP are also examined. The Inner TP contains the largest number of lakes (55.03 %), the greatest total lake area ((28,416.77 ± 255.69) km², 66 %), and the largest lake density (0.026/km²). The Yellow River and Yangtze River basins also have a large number of lakes (>10 % of the total,

each). Lakes are mostly concentrated at a latitude of 34°N in terms of number, and 31°N in terms of total area. The lake database provided by this study has important implications for future studies, and may be used in water balance estimations, studies of lake level changes based on satellite altimetry data, and assessment of biogeochemical cycling.

The lake abundance and size distributions are evaluated for each basin and for the entire TP. Lakes at the mean elevation ($n = 53$, mean elevation = 4,715 m) conform closely to a power-law distribution with an r^2 value of 0.97 and a slope of -0.66, which fall within the critical value and the theoretical constraints for such a relationship.

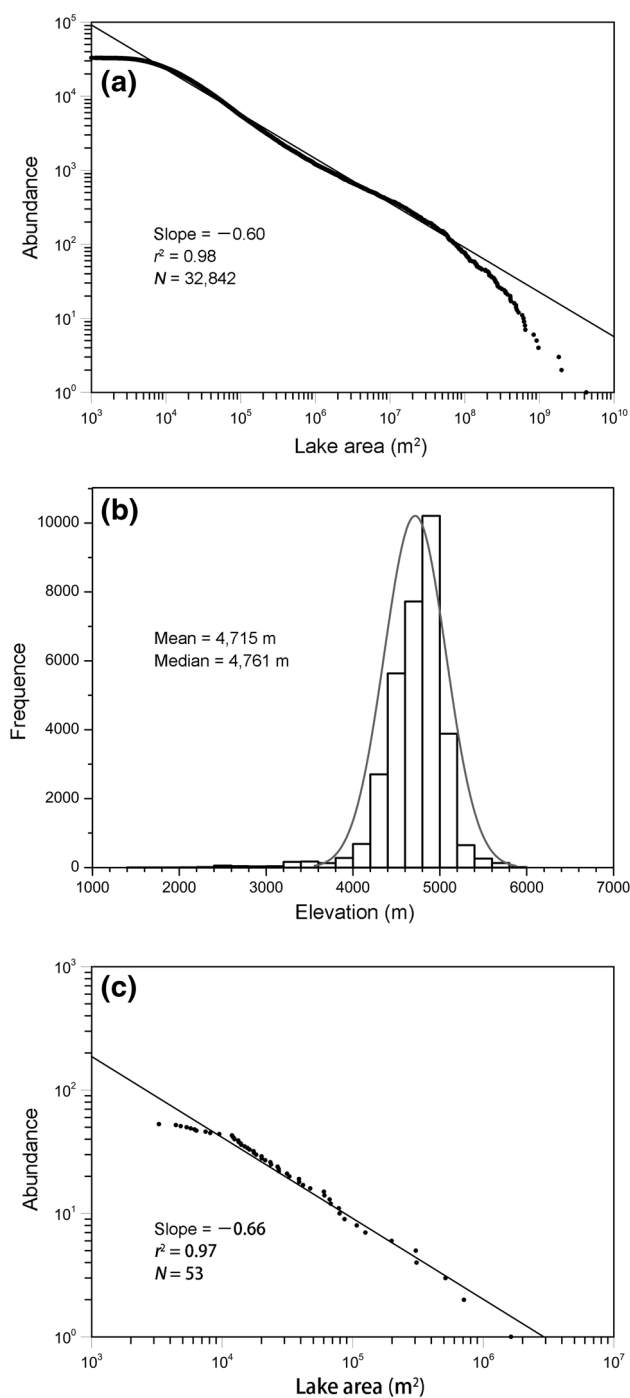


Fig. 8 Log-abundance versus log-size plot for lakes in the TP. **a** all lakes derived from Landsat mosaic 2000, **b** histogram of elevation distribution for all lakes, and **c** lakes at the mean elevation (4,715 m)

However, lakes located across all basins over the entire TP do not follow such a power-law distribution. This is consistent with the results obtained by [5] that the power-law distribution assumption for mountain ranges may have overestimated lake numbers and lake areas. However, the slopes of all distribution plots are larger than -1 , further supporting the concept that larger lakes, rather than small

lakes, contribute more to the total lake surface area in a region. In the present study, lake data has been truncated with a lower area limit of 0.001 km^2 . Future lake inventories may be updated using satellite data with higher spatial resolutions, when available across the entire TP.

Acknowledgements This work was supported by the National Natural Science Foundation of China (41301063, 41190081, and 31228021), and the Strategic Priority Research Program (B) of the Chinese Academy of Sciences (XDB01020300). Landsat GeoCover mosaics provided by the University of Maryland's Global Land Cover Facility (<http://glcf.umd.edu/data/mosaic/>), Landsat TM/ETM+ from Geospatial Data Cloud, Computer Network Information Center, Chinese Academy of Sciences at <http://www.gscloud.cn> and USGS at <http://glovis.usgs.gov/> were sincerely acknowledged.

References

1. Krinner G (2003) Impact of lakes and wetlands on boreal climate. *J Geophys Res* 108:4520
2. Cole JJ, Prairie YT, Caraco NF et al (2007) Plumbing the global carbon cycle: integrating inland waters into the terrestrial carbon budget. *Ecosystems* 10:172–185
3. Tranvik LJ, Downing JA, Cotner JB et al (2009) Lakes and reservoirs as regulators of carbon cycling and climate. *Limnol Oceanogr* 54:2298–2314
4. Lehner B, Döll P (2004) Development and validation of a global database of lakes, reservoirs and wetlands. *J Hydrol* 296:1–22
5. Seekell DA, Pace ML, Tranvik LJ et al (2013) A fractal-based approach to lake size-distributions. *Geophys Res Lett* 40:517–521
6. McDonald CP, Rover JA, Stets EG et al (2012) The regional abundance and size distribution of lakes and reservoirs in the United States and implications for estimates of global lake extent. *Limnol Oceanogr* 57:597–606
7. Downing JA, Prairie Y, Cole J et al (2006) The global abundance and size distribution of lakes, ponds, and impoundments. *Limnol Oceanogr* 51:2388–2397
8. Seekell DA, Pace ML (2011) Does the Pareto distribution adequately describe the size-distribution of lakes? *Limnol Oceanogr* 56:350–356
9. Balcerak E (2013) How many lakes are there, and how big are they? *Eos Trans Amer Geophys Union* 94:104–214
10. Lewis WM (2011) Global primary production of lakes: 19th Baldi Memorial Lecture. *Inland Waters* 1:1–28
11. Meybeck M (1995) Global distribution of lakes. In: Vorosmarty C (ed) *Physics and chemistry of lakes*. Springer, Heidelberg, pp 1–35
12. Yao T, Thompson L, Yang W et al (2012) Different glacier status with atmospheric circulations in Tibetan Plateau and surroundings. *Nat Clim Change* 2:663–667
13. Gardner AS, Moholdt G, Cogley JG et al (2013) A reconciled estimate of glacier contributions to sea level rise: 2003–2009. *Science* 340:852–857
14. Liu XD, Chen BD (2000) Climatic warming in the Tibetan Plateau during recent decades. *Int J Climatol* 20:1729–1742
15. Zhang G, Xie H, Duan S et al (2011) Water level variation of Lake Qinghai from satellite and in situ measurements under climate change. *J Appl Remote Sens* 5:053532
16. Zhang G, Xie H, Kang S et al (2011) Monitoring lake level changes on the Tibetan Plateau using ICESat altimetry data (2003–2009). *Remote Sens Environ* 115:1733–1742

17. Zhang G, Xie H, Yao T et al (2012) Snow cover dynamics of four lake basins over Tibetan Plateau using time series MODIS data (2001–2010). *Water Resour Res* 48:W10529
18. Zhang G, Yao T, Xie H et al (2013) Increased mass over the Tibetan Plateau: from lakes or glaciers? *Geophys Res Lett* 40: 2125–2130
19. Zhang G, Xie H, Yao T et al (2013) Water balance estimates of ten greatest lakes in China using ICESat and Landsat data. *Chin Sci Bull* 58:3815–3829
20. Phan VH, Lindenbergh R, Menenti M (2012) Icesat derived elevation changes of Tibetan lakes between 2003 and 2009. *Int J Appl Earth Obs Geoinf* 17:12–22
21. Wang X, Gong P, Zhao Y et al (2013) Water-level changes in China's large lakes determined from ICESat/GLAS data. *Remote Sens Environ* 132:131–144
22. Sun F, Zhao Y, Gong P et al (2013) Monitoring dynamic changes of global land cover types: fluctuations of major lakes in China every 8 days during 2000–2010. *Chin Sci Bull* 59:171–189
23. Yang K, Ye B, Zhou D et al (2011) Response of hydrological cycle to recent climate changes in the Tibetan Plateau. *Clim Change* 109:517–534
24. Lei Y, Yao T, Bird BW et al (2013) Coherent lake growth on the central Tibetan Plateau since the 1970s: characterization and attribution. *J Hydrol* 483:61–67
25. Hanson PC, Carpenter SR, Cardille JA et al (2007) Small lakes dominate a random sample of regional lake characteristics. *Freshw Biol* 52:814–822
26. Ma R, Yang G, Duan H et al (2011) China's lakes at present: number, area and spatial distribution. *Sci China Earth Sci* 54: 283–289
27. Wang SM, Dou HS (1998) Chinese lakes inventory. Institute of Geography and Limnology, Beijing
28. Ma R, Duan H, Hu C et al (2010) A half-century of changes in China's lakes: global warming or human influence? *Geophys Res Lett* 37:24106
29. Zhu D, Meng X, Zheng D et al (2007) Changes of rivers and lakes on the Qinghai-Tibet Plateau in the past 25 years and their influence factors. *Geol Bull Chin* 26:22–30
30. Yao T, Pu J, Lu A et al (2007) Recent glacial retreat and its impact on hydrological processes on the Tibetan Plateau, China, and surrounding regions. *Arctic Antarctic Alpine Res* 39:642–650
31. Zhu LP, Xie MP, Wu YH (2010) Quantitative analysis of lake area variations and the influence factors from 1971 to 2004 in the Nam Co basin of the Tibetan Plateau. *Chin Sci Bull* 55:1294–1303
32. Nie Y, Zhang Y, Ding M et al (2013) Lake change and its implication in the vicinity of Mt. Qomolangma (Everest), central high Himalayas, 1970–2009. *Environ Earth Sci* 68:251–265
33. Song C, Huang B, Ke L (2013) Modeling and analysis of lake water storage changes on the Tibetan Plateau using multi-mission satellite data. *Remote Sens Environ* 135:25–35
34. Farr TG, Rosen PA, Caro E et al (2007) The Shuttle Radar Topography Mission. *Rev Geophys* 45:4001
35. Valeriano MM, Kuplich TM, Storino M et al (2006) Modeling small watersheds in Brazilian Amazonia with Shuttle Radar Topographic Mission-90 m data. *Comput Geosci* 32:1169–1181
36. Tucker CJ, Grant DM, Dykstra JD (2004) NASA's global orthorectified Landsat data set. *Photogramm Eng Remote Sens* 70:313–322
37. Koeln G, Dykstra J, Cunningham J (1999) Geocover and geocover-1c: orthorectified Landsat TM/MSS data and derived land cover for the world. In: Proceedings of international symposium on digital earth, Western Australia University, Crawley 23–25 August 1999
38. USGS (2004) Phase 2 gap-fill algorithm: slc-off gap-filled products gap-fill algorithm methodology. Landsat.usgs.gov/documents/L7SLCGapFilledMethod.pdf. Accessed 10 Aug 2013
39. Verpoorter C, Kutser T, Tranvik L (2012) Automated mapping of water bodies using Landsat multispectral data. *Limnol Oceanogr* 10:1037–1050
40. Feyisa GL, Meilby H, Fensholt R et al (2014) Automated water extraction index: a new technique for surface water mapping using landsat imagery. *Remote Sens Environ* 140:23–35
41. Xu H (2006) Modification of normalised difference water index (NDWI) to enhance open water features in remotely sensed imagery. *Int J Remote Sens* 27:3025–3033
42. Fujita K, Sakai A, Nuimura T et al (2009) Recent changes in Imja glacial lake and its damming moraine in the Nepal Himalaya revealed by in situ surveys and multi-temporal ASTER imagery. *Environ Res Lett* 4:045205
43. Salerno F, Thakuri S, D'Agata C et al (2012) Glacial lake distribution in the Mount Everest region: uncertainty of measurement and conditions of formation. *Glob Planet Change* 92:30–39
44. Hamilton SK, Melack JM, Goodchild MF et al (1992) Estimation of the fractal dimension of terrain from lake size distributions. In: Lewis WM (ed) Lowland floodplain rivers: geomorphological perspectives. Wiley, Chichester, pp 145–163
45. Goodchild MF (1998) Lakes on fractal surfaces: a null hypothesis for lake-rich landscapes. *Math Geol* 20:615–630
46. Bolch T, Yao T, Kang S et al (2010) A glacier inventory for the western Nyainqêntanglha range and Nam Co basin, Tibet, and glacier changes 1976–2009. *Cryosphere* 4:419–433
47. Kang SC, Chen F, Ye QH et al (2007) Glacier retreating dramatically on the Mt. Nyainqêntanglha during the last 40 years. *J Glaciol Geocryol* 29:869–873 (in Chinese)
48. Yao T, Li Z, Yang W et al (2010) Glacial distribution and mass balance in the Yarlung Zangbo River and its influence on lakes. *Chin Sci Bull* 55:2072–2078
49. Xu ZX, Gong TL, Li JY (2008) Decadal trend of climate in the Tibetan Plateau—regional temperature and precipitation. *Hydrol Process* 12:3056–3065
50. Zhou S, Kang S, Chen F et al (2013) Water balance observations reveal significant subsurface water seepage from lake Nam Co, south-central Tibetan Plateau. *J Hydrol* 491:89–99
51. Bian D, Du J, Hu J et al (2009) Response of the water level of the Yamzho Yumco to climate change during 1975–2006. *J Glaciol Geocryol* 31:404–409 (in Chinese)
52. Liu-Zeng J, Tapponnier P, Gaudemer Y et al (2008) Quantifying landscape differences across the Tibetan Plateau: implications for topographic relief evolution. *J Geophys Res* 113:F04018
53. Liu J, Ding L, Zeng L et al (2006) Large-scale terrain analysis of selected regions of the Tibetan Plateau: discussion on the origin of plateau planation surface. *Earth Sci Front* 13:285–299
54. Chen Y, Zong Y, Li B et al (2013) Shrinking lakes in Tibet linked to the weakening asian monsoon in the past 8.2 ka. *Quat Res* 80: 189–198
55. Xu W, Florian S, Ai-guo Z et al (2013) Glacier and glacial lakes changes and their relationship in the context of climate change, central Tibetan Plateau 1972–2010. *Glob Planet Change* 111:246–257
56. Li J, Sheng Y (2012) An automated scheme for glacial lake dynamics mapping using landsat imagery and digital elevation models: a case study in the Himalayas. *Int J Remote Sens* 33: 5194–5213
57. Wang W, Yao T, Yang W et al (2012) Methods for assessing regional glacial lake variation and hazard in the southeastern Tibetan Plateau: a case study from the Boshula mountain range, China. *Environ Earth Sci* 67:1441–1450